



HAL
open science

Influence of spacer in the formation of nanorings by templateless electropolymerization

Fatoumata Sow, Abdoulaye Dramé, Salif Sow, Aboubacary Sene, François Orange, Samba Yandé Dieng, Frédéric Guittard, Thierry Darmanin

► **To cite this version:**

Fatoumata Sow, Abdoulaye Dramé, Salif Sow, Aboubacary Sene, François Orange, et al.. Influence of spacer in the formation of nanorings by templateless electropolymerization. *Materials Today Chemistry*, 2020, 10.1016/j.mtchem.2020.100278 . hal-03554149

HAL Id: hal-03554149

<https://hal.science/hal-03554149>

Submitted on 3 Feb 2022

HAL is a multi-disciplinary open access archive for the deposit and dissemination of scientific research documents, whether they are published or not. The documents may come from teaching and research institutions in France or abroad, or from public or private research centers.

L'archive ouverte pluridisciplinaire **HAL**, est destinée au dépôt et à la diffusion de documents scientifiques de niveau recherche, publiés ou non, émanant des établissements d'enseignement et de recherche français ou étrangers, des laboratoires publics ou privés.

Influence of spacer in the formation of nanorings by templateless electropolymerization

Fatoumata Sow^a, Abdoulaye Dramé^a, Salif Sow^a, Aboubacary Sene^a, François Orange^b, Samba Yandé Dieng^a, Frédéric Guittard^{c,d} and Thierry Darmanin^{c,*}

^a*Université Cheikh Anta Diop, Faculté des Sciences et Techniques, Département de Chimie, B.P. 5005 Dakar, Sénégal.*

^b*Université Côte d'Azur, CCMA, 06100, Nice, France.*

^c*Université Côte d'Azur, NICE Lab, IMREDD, 61-63 Av. Simon Veil, 06200 Nice, France.*

Corresponding author: thierry.darmanin@unice.fr

^d*University California Riverside, Department of Bioengineering, Riverside, CA, USA*

Abstract

In this original work, we want to control the shape of the resulting porous structures by templateless electropolymerization, by adjusting the spacer (alkyl chains or aromatic groups) between thieno[3,4-*b*]thiophene and carbazole used as the monomer and the substituent, respectively. A huge change is especially observed from ribbon-like structures to nanorings as the alkyl spacer increases. The presence of a significant amount of water is necessary for the formation of these porous structures because it allows releasing a high amount of gas bubbles. The size and number of nanorings are dependent on both the alkyl spacer and electrochemical parameters such as the number of deposition scans. These surfaces could be used in the future in various potential applications such as in water harvesting, oil/water separation membranes, optical devices, sensors or photocatalysis.

Keywords: Nanostructure, Conducting polymers, Electrochemistry, Bioinspiration, Wettability

Introduction

Beyond their overall impact on surface properties and applications in interfacial engineering, well-controlled surface structures are also omnipresent in nature such as in gecko toepads, plants and leaf surfaces [1–6]. The influence in the shape control on surface nanostructures is fundamental for various applications especially in sensors, photocatalysis, energy systems, drug delivery, and surface wettability [7–14].

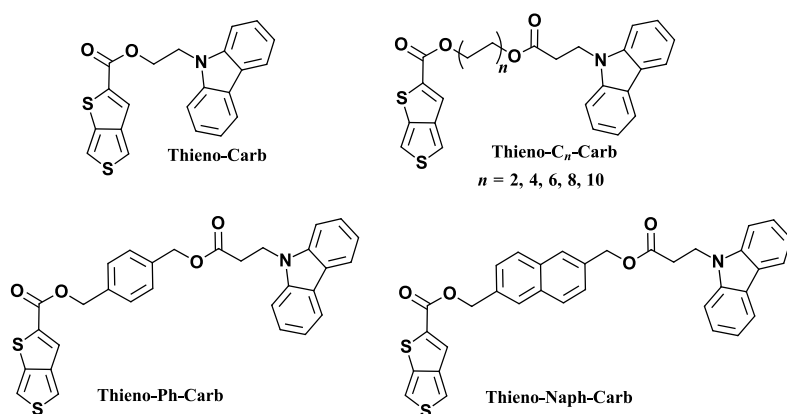
The preparation of well-ordered surface nanoporous structures have typically been made using lithographic process or using hard templates, such as anodized aluminum oxide (AAO) membranes which specifically direct the formation of surface features [15–19]. These strategies are quite labor-intensive and with hard templates, the membranes are often “single-use” when we want to investigate various nanostructure geometrical parameters (e.g. height, diameter, etc.).

Templateless electropolymerization is a very versatile alternative to prepare very quickly very ordered structures of controllable size but also shape (nanotubes, nanoribbons, hollow nanospheres...)[20–35]. For example, the templateless electropolymerization of pyrrole in water (H₂O) has been specifically studied and it was demonstrated that the formation of porous structures is possible when gas bubbles are released: here, H₂ and/or O₂ from H₂O depending on the polymerization process [20–26]. However, a surfactant is necessary to stabilize the gas bubbles and induce the polymer growth around them. Moreover, most of the monomers are not soluble in water.

It was very recently demonstrated that organic solvents of lower polarity such as dichloromethane (CH₂Cl₂) can be used. Exceptional results without surfactant were reported with very rigid and aromatic monomers such as 3,4-phenylenedioxythiophene (PheDOT), 3,4-naphthalenedioxythiophene (NaphDOT) or thieno[3,4-*b*]thiophene derivatives, allowing high π -sticking interactions [27–36]. These structures can be produced even at low H₂O content (H₂O naturally present in solution) even if H₂O content has often a huge influence for example on the structure shape or the number of nanotubes.

Thieno[3,4-*b*]thiophene was found to be an exceptional monomer leading to polymer with unique opto-electronical properties [37–40] while this structure could lead to various

nanostructures with this technique [31–35]. Using thieno[3,4-*b*]thiophene-based monomers, it was also previously reported unique results with carbazole [32] as the substituent because it participates to electropolymerization and also induces high π -sticking interaction. In this original work, we have wanted to investigate how a spacer (alkyl or aromatic) between the monomer core and the substituent (Scheme 1) can affect the polymer growth around gas bubbles leading to different structure shapes, particularly nanorings. It is worth noting that nanorings are difficult to produce by templateless electropolymerization [41–46] while these nanomaterials are expected especially for their optical properties [42]. Here, two different solvents are investigated: CH_2Cl_2 and CH_2Cl_2 saturated with H_2O (named here $\text{CH}_2\text{Cl}_2 + \text{H}_2\text{O}$). Indeed, it was shown that H_2O content has a huge influence in the formation of porous structures but affects especially the number of porous structures not their shape. [35]. This is why here, in order to investigate the effect of the spacer on the structure shape, it was chosen to test only these two solvents (CH_2Cl_2 and $\text{CH}_2\text{Cl}_2 + \text{H}_2\text{O}$).

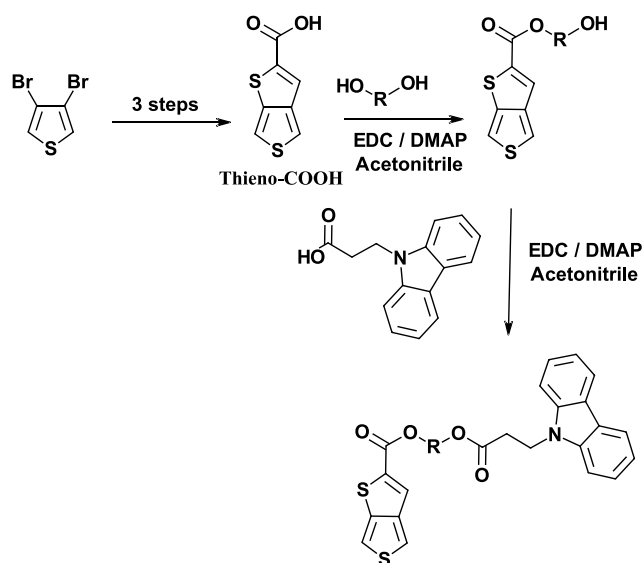


Scheme 1. Investigated monomers in this original paper.

2. Experimental Section

2-(9*H*-carbazol-9-yl)ethyl thieno[3,4-*b*]thiophene-2-carboxylate (Thieno-Carb) was synthesized using a previously reported procedure [32]. For the other original monomers, thieno[3,4-*b*]thiophene-2-carboxylic acid (Thieno-COOH) was synthesized in three steps from 3,4-dibromothiophene (Scheme 2) [37–38]. More precisely, 1.0 eq (200 mg) of Thieno-COOH was dissolved in 20 mL of anhydrous acetonitrile in a 100 mL flask in the presence of 1.2 eq of EDC and 20 mg of DMAP (1.6 %). After stirring for 30 mn, 1.5 eq of the corresponding diol was added previously dissolved in acetonitrile. After 24 h, the products

were purified by column chromatography on silica gel (ether / cyclohexane as eluant) to obtain the alcohols.



Scheme 2. Synthesis way to the monomers.

Thieno-C₂-OH: 2-hydroxyethyl thieno[3,4-*b*]thiophene-2-carboxylate. Yield 58%; Liquid; δ_{H} (400 MHz, CDCl_3): 7.74 (s, 1H), 7.61 (d, 1H, $J = 2.4$ Hz), 7.30 (dd, $J = 2.7$ Hz, $J = 0.8$ Hz, 1H), 4.47 (t, $J = 4.4$ Hz, 2H), 3.95 (m, 2H), 2.05 (s, 1H); δ_{C} (400 MHz, CDCl_3): 163.36, 145.77, 139.72, 138.92, 124.08, 116.96, 111.47, 65.14, 61.21.

Thieno-C₄-OH: 4-hydroxybutyl thieno[3,4-*b*]thiophene-2-carboxylate. Yield 21%; Liquid; δ_{H} (400 MHz, CDCl_3): 7.71 (s, 1H), 7.60 (d, $J = 2.4$ Hz, 1H), 7.29 (dd, $J = 2.7$ Hz, $J = 1.0$ Hz, 1H), 4.36 (t, 2H, $J = 6.4$ Hz), 3.74 (t, $J = 6.4$ Hz, 2H), 3.08 (s, 1H), 1.87 (m, 2H), 1.73 (m, 2H); δ_{C} (400 MHz, CDCl_3): 163.16, 145.91, 139.15, 123.59, 116.72, 111.41, 65.40, 62.38, 29.17, 25.18.

Thieno-C₆-OH: 6-hydroxyhexyl thieno[3,4-*b*]thiophene-2-carboxylate. Yield 26%; Liquid; δ_{H} (400 MHz, CDCl_3): 7.63 (s, 1H), 7.53 (d, $J = 2.4$ Hz, 1H), 7.22 (dd, $J = 2.7$ Hz, $J = 0.8$ Hz, 1H), 4.25 (t, $J = 6.4$ Hz, 2H), 3.60 (t, $J = 6.4$ Hz, 2H), 1.79 (m, 2H), 1.61 (m, 2H), 1.47 (s, 1H), 1.43 (m, 5H); δ_{C} (400 MHz, CDCl_3): 163.20, 145.93, 139.78, 123.47, 116.61, 111.35, 65.53, 62.81, 32.58, 28.59, 25.73, 25.36.

Thieno-C₈-OH: 8-hydroxyoctyl thieno[3,4-*b*]thiophene-2-carboxylate. Yield 20%; Liquid; δ_{H} (400 MHz, CDCl_3): 7.70 (s, 1H), 7.60 (d, $J = 2.6$ Hz, 1H), 7.28 (dd, $J = 2.7$ Hz, $J = 0.8$ Hz, 1H), 4.32 (t, $J = 6.6$ Hz, 2H), 3.63 (t, $J = 6.4$ Hz, 2H), 1.75 (m, 2H), 1.60 (m, 2H), 1.45 (m,

8H); δ_{C} (400 MHz, CDCl_3): 163.21, 145.94, 139.81, 123.45, 116.61, 111.36, 65.70, 63.02, 32.74, 29.28, 29.18, 28.62, 25.87, 25.65.

Thieno-C₁₀-OH: 10-hydroxydecyl thieno[3,4-*b*]thiophene-2-carboxylate. Yield 25%; Liquid; δ_{H} (400 MHz, CDCl_3): 7.70 (s, 1H), 7.60 (d, $J = 3.2$ Hz, 1H), 7.29 (dd, $J = 2.7$ Hz, $J = 0.8$ Hz, 1H), 4.30 (t, $J = 6.6$ Hz, 2H), 3.64 (t, $J = 6.4$ Hz, 2H), 1.75 (m, 2H), 1.56 (m, 2H), 1.40 (m, 12H); δ_{C} (400 MHz, CDCl_3): 163.21, 145.94, 139.84, 123.42, 116.58, 111.36, 65.70, 63.08, 32.74, 29.28, 29.18, 28.62, 25.92, 25.91, 25.87, 25.72.

Thieno-Ph-OH: 2-hydroxyethyl thieno[3,4-*b*]thiophene-2-carboxylate. Yield 36%; Liquid; δ_{H} (400 MHz, CDCl_3): 7.75 (s, 1H), 7.60 (d, $J = 4.2$, 1H), 7.42 (d, $J = 8.4$ Hz, 4H), 7.35 (s, 1H), 7.26 (dd, $J = 1.4$ Hz, $J = 1.7$ Hz, 1H), 6.98 (s, 1H), 5.35 (s, 2H), 2.05 (s, 1H), 4.71 (s, 1H), 2.25 (s, 1H); δ_{C} (400 MHz, CDCl_3): 162.99, 141.16, 135.79, 134.97, 128.51, 127.22, 125.53, 123.93, 111.44, 66.93, 65, 30.34.

Thieno-Naph-OH: 2-hydroxyethyl thieno[3,4-*b*]thiophene-2-carboxylate. Yield 14%; Liquid; δ_{H} (400 MHz, CDCl_3): 7.89 (s, 2H), 7.84 (d, $J = 4.4$ Hz, 2H), 7.76 (s, 1H), 7.60 (d, $J = 4.7$ Hz, 1H), 7.53 (d, $J = 3$ Hz, 2H), 7.3 (s, 1H), 5.52 (s, 2H), 4.88 (s, 2H), 2.25 (s, 1H); δ_{C} (400 MHz, CDCl_3): 171.48, 140, 139.91, 135.79, 125.99, 125.79, 123.1, 122.92, 119.40, 119.2, 108.97, 60.93, 38.77, 30.75.

The monomers were synthesized by reacting 3-(9*H*-carbazol-9-yl)propanoic acid and the intermediates molecules via a simple esterification reaction (Scheme 2). Briefly 1.2 eq of 3-(9*H*-carbazol-9-yl)propanoic acid was dissolved in 20 mL of acetonitrile in the presence of 1.2 eq of EDC and 20 mg of DMAP or (1.6 mmol) with stirring at room temperature for 30 minutes. Then, the intermediate molecule dissolved in acetonitrile was added. After 24 hours, the products were purified by chromatography on a column of silica gel (ether / cyclohexane, as eluent).

Thieno-C₂-Carb: 2-hydroxyethyl thieno[3,4-*b*]thiophene-2-carboxylate. Yield 56%; Liquid; δ_{H} (400 MHz, CDCl_3): 8.08 (d, $J = 15.2$ Hz, 2H), 7.65 (s, 1H), 7.60 (d, $J = 5.6$ Hz, 1H), 7.45 (m, 4H), 7.24 (m, 3H), 4.67 (t, $J = 7.0$ Hz, 2H), 4.38 (dd, $J = 3.6$ Hz, $J = 10.4$ Hz, 4H), 2.92 (t, $J = 7.2$ Hz, 2H); δ_{C} (400 MHz, CDCl_3): 171.15, 162.75, 145.79, 139.92, 125.79, 124.10, 123.10, 120.41, 119.22, 126.51, 126.10, 125.85, 125.39, 125.35, 124.01, 123.34, 123.19, 123.10, 122.96, 122.73, 116.99, 111.45, 108.55, 62.82, 62.39, 29.70.

Thieno-C₄-Carb: 4-hydroxybutyl thieno[3,4-*b*]thiophene-2-carboxylate. Yield 18%; Liquid; δ_{H} (400 MHz, CDCl_3): 8.10 (d, $J = 15.2$ Hz, 2H), 7.68 (s, 1H), 7.60 (d, $J = 5.2$ Hz, 1H), 7.47

(m, 4H) 7.29 (m, 3H), 4.66 (t, J = 7.0 Hz, 2H), 4.22 (t, J = 4.0 Hz, 2H), 4.09 (t, J=6.0 Hz,2H), 2.86 (t, J = 7.0 Hz, 2H), 1.25 (m, 4H); δ_C (400 MHz, CDCl₃): 171.53, 139.94, 125.79, 123.61, 123.07, 120.39, 119.22, 116.73, 111.41, 108.60, 64.36, 38.80, 33.55, 25.11, 25.04.

Thieno-C₆-Carb: 6-hydroxyhexyl thieno[3,4-*b*]thiophene-2-carboxylate. Yield 15%; Liquid; δ_H (400 MHz, CDCl₃): 8.10 (d, J = 15.6 Hz, 2H), 7.68 (s, 1H), 7.58 (d, J = 5.2 Hz, 1H), 7.47 (m, 4H), 7.20 (m, 3H), 4.64 (t, J = (5.9 Hz, 2H), 4.26 (t, J = 5.5Hz, 2H), 4.00 (t, J = 5.5 Hz, 2H), 2.84 (t, J = 5.9 Hz, 2H), 1.32 (m, -H); δ_C (400 MHz, CDCl₃): 145.89, 140, 125.80, 123.51, 123.08, 120.39, 119.21, 116.67, 111.39, 108.64, 65.47, 64.89, 39.67, 38.84, 33.60,28.45, 28.29, 25.56, 25.44.

Thieno-C₈-Carb: 8-hydroxyoctyl thieno[3,4-*b*]thiophene-2-carboxylate. Yield 35%; Liquid; δ_H (400 MHz, CDCl₃): 7.92 (d, J =15.6 Hz, 2H), 7.50 (s, 1H), 7.39 (d, J = 5.6 Hz, 1H), 7.29 (m, 4H), 7.12 (m, 3H), 4.48 (t, J = 7.0 Hz, 2H), 4.14 (t, J = 6.8 Hz, 2H), 3.85 (t, J = 6.6 Hz, 2H), 2.69 (t, J = 7.0 Hz, 2H), 1.58 (m, 4H), 1.3 (m, 8H); δ_C (400 MHz, CDCl₃): 171.60, 163.19, 145.94, 140.02, 139.80, 125.81, 123.47, 123.10, 120.41, 119.22, 116.66, 111.40, 108.67, 77.74, 77.11, 76.47, 65.68, 65.08, 53.50, 124.88, 123.46, 38.83, 33.61, 29.05, 28.62, 28.39, 25.84, 25.70.

Thieno-C₁₀-Carb: 10-hydroxydecyl thieno[3,4-*b*]thiophene-2-carboxylate. Yield 74%; Liquid; δ_H (400 MHz, CDCl₃): 7.83 (d, J= 15.2 Hz, 2H), 7.50 (s, 1H), 7.39 (d, J = 5.6 Hz, 1H), 7.30 (m, 4H), 6.90 (m, 3H), 4.40 (t, J = 13.2 Hz, 2H), 3.98 (t, J = 6.4 Hz, 2H), 3.54 (t, J = 6.4 Hz,2H), 2.53 (t, J = 6.6 Hz, 2H), 2.20 (m, 2H), 1.37 (m, 2H), 1.66 (m, 12H); δ_C (400 MHz, CDCl₃): 176.43, 167.65, 150.62, 144.87, 143.68, 130.87, 127.45, 125.41, 124.11, 124.04, 114.54, 38.53, 34.00, 33.77, 33.01, 31.56, 30.36., 25.72.

Thieno-Ph-Carb: 2-hydroxyethyl thieno[3,4-*b*]thiophene-2-carboxylate. Yield 30.48%; Liquid; δ_H (400 MHz, CDCl₃): 8.11 (d, J = 15.6 Hz, 2H), 7.73 (d, J =1.2 Hz, 1H), 7.59 (d, J = 5.6 Hz, 1H), 7.26 (m, 9H), 7.14 (s, 1H), 7.01 (s, 1H), 5.34 (s, 2H), 5.06 (s, 2H), 4.66 (t, J = 7.0 Hz, 2H), 2.93 (t, J = 7.0 Hz, 2H); δ_C (400 MHz, CDCl₃): 171.31, 162.94, 145.88, 140, 135.79, 125.88, 124.02, 123.16, 120.47, 119.30, 116.96, 111.51, 108.67, 66.76, 38.77, 34.30, 30.4, 26.99.

Thieno-Naph-Carb: 2-hydroxyethyl thieno[3,4-*b*]thiophene-2-carboxylate. Yield 43.79%; Liquid; δ_H (400 MHz, CDCl₃): 7.87 (d, J = 1.4 Hz, 2H), 7.7 (s, 1H), 7.65 (dd, J = 4.8 Hz J = 17.2 Hz, 2H), 7.58 (d, J = 1.2 Hz, 1H), 7.5 (s, 1H), 7.4 (d, J = 5.6 Hz, 1H), 7.35 (dd, J = 3.6Hz, J=17.2Hz, 1H), 7.28 (m, 4H), 7.15 (m, 4H), 5.33 (s, 2H), 5.02 (s, 2H), (t, J = 7.2 Hz, 2H), 2.79 (t, J = 7.2 Hz, 2H); δ_C (400 MHz, CDCl₃): 163.40, 145.81, 139.15, 138.95, 124.12, 117.00, 111.51, 65.7, 61.25.

2.2. Electropolymerization parameters

In agreement with previous works [35], two solvents were studied here: dichloromethane (CH_2Cl_2) and dichloromethane saturated with water ($\text{CH}_2\text{Cl}_2 + \text{H}_2\text{O}$). Here, it was chosen to saturate CH_2Cl_2 with H_2O because of the low solubility of H_2O in CH_2Cl_2 (typically around 0.15 g/100 mL). $\text{CH}_2\text{Cl}_2 + \text{H}_2\text{O}$ was simply prepared by mixing CH_2Cl_2 with a high amount of H_2O and discarding the aqueous phase after decantation. Tetrabutylammonium perchlorate (Bu_4NClO_4) (0.1 M) was chosen as exceptional electrolyte for these experiments. Then, each monomer (0.01 M) was added separately. The electropolymerization experiments were done with an Autolab potentiostat and using three electrodes: 2 cm² gold-coated silicon wafer as the working electrode, a carbon rod as the counter-electrode and a saturated calomel electrode (SCE) as the reference electrode. The monomer oxidation potentials (E^{ox}) were first determined by cyclic voltammetry. Then, the depositions were performed by cyclic voltammetry (1, 3 and 5 scans) from -1 V to E^{ox} at a scan rate of 20 mV s⁻¹. After, the substrates were washed three times in CH_2Cl_2 and slowly dried.

2.3 Surface properties

The surfaces structures were obtained *via* scanning electron microscopy (SEM) (6700F microscope from JEOL). The surface hydrophobicity was characterized *via* goniometer (DSA30 from Bruker) with 2 μL water droplets and by measuring the apparent contact angles with water (θ_w) taken at the triple point (n=5). The arithmetic (Ra) and quadratic (Rq) surface roughness were determined *via* optical profiling system (WYKO NT1100 from Bruker). The measurements were realized with the working mode High Mag Phase Shift Interference (PSI), the objective 20X, and the field of view 0.5X. For EDX analyses, samples were analyzed with a Tescan Vega 3 XMU scanning electron microscope (TESCAN FRANCE, Fuveau, France) equipped with an X-MaxN 50 EDX detector (Oxford Instruments, Abingdon, U.K.). Samples were carbon-coated prior to analyses. All analyses were performed under identical conditions: an acceleration voltage of 10 kV, a 10 mm working distance and a 2000 \times magnification. EDX spectra were processed with the Aztec software (version 3.1, Oxford Instruments).

3. Result and Discussion

3.1. Templateless electropolymerization and electrochemical characterization

First, the influence of H₂O in this process was characterized. Because, H₂O can be oxidized or reduced to form O₂ and H₂, respectively at different potentials, the two solvents were electrochemically characterized by varying the potential range (cyclic voltammetry). The cyclic voltammograms of CH₂Cl₂ and CH₂Cl₂ + H₂O are gathered in Figure 1.

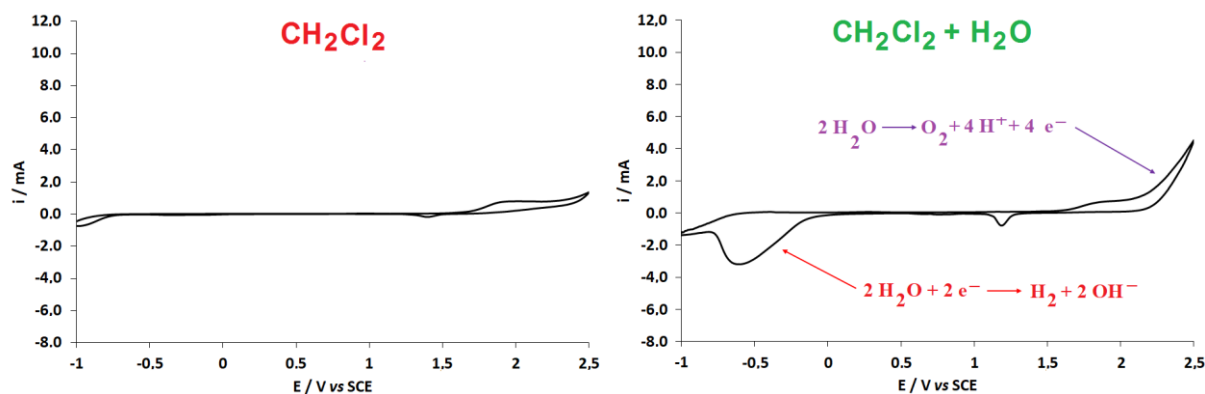


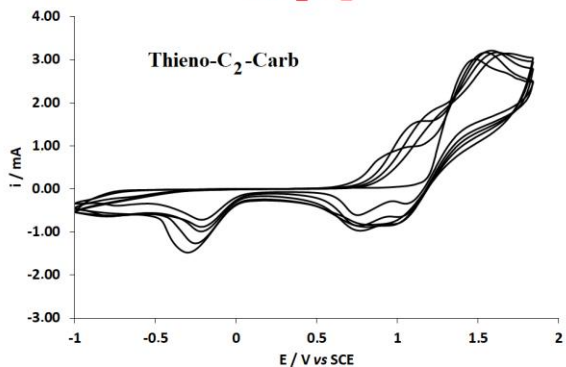
Figure 1. Cyclic voltammogram of CH₂Cl₂ (left) and CH₂Cl₂ + H₂O (right) with 0.1 M Bu₄NClO₄ at a scan rate 20 mV s⁻¹ (1 scan).

The cyclic voltammogram of CH₂Cl₂ + H₂O clearly displays a large peak at ≈ -0.5 V vs during the back scan confirming the reaction $2 \text{H}_2\text{O} + 2 \text{e}^- \rightarrow \text{H}_2$ (bubbles) + 2OH^- . The peak starts at ≈ -0.0 V and extends to ≈ -0.85 V. Another peak is also present during the forward scan, indicative of the reaction $2 \text{H}_2\text{O} \rightarrow \text{O}_2$ (bubbles) + $4 \text{H}^+ + 4 \text{e}^-$ but this one starts only at ≈ 2.0 V vs SCE. After adding the monomers, the monomer oxidation potential (E^{ox}) were found to be roughly 1.80-1.90 V vs SCE. Then, the polymers were electrodeposited by cyclic voltammetry from -1 V to E^{ox} . In this potential range, the release of H₂ bubbles is mainly expected. In order to investigate the polymer growth, the polymers were electrodeposited at scan rate of 20 mV s⁻¹ and using three different numbers of scan: 1, 3 and 5.

Examples of cyclic voltammograms of different monomers and the two solvents are given in Figure 2. The polymers display oxidation and reduction peaks within the range 0.5-1.5 V. Usually, the cyclic voltammetry curves for these monomers do not superpose after each scan indicating that the substituent has significant steric hindrance whatever the spacer. However, the intensity of the curves is high indicating of important thickness, except with the longest alkyl chain (**Thieno-C₁₀-Carb**). Indeed, it is expected in CH₂Cl₂ that polymer solubility should increase with the alkyl spacer.

In $\text{CH}_2\text{Cl}_2 + \text{H}_2\text{O}$, the cyclic voltammograms are different but these polymers have a good resistance to the pressure induced by the gas bubbles released during the process, compared to other substituents used in the literature [31,32]. Indeed, as reported in the literature, carbazole participates significantly in the polymerization because it has an oxidation potential close to that of thieno[3,4-*b*]thiophene, and also can induce high π -stacking interactions.

CH₂Cl₂



CH₂Cl₂ + H₂O

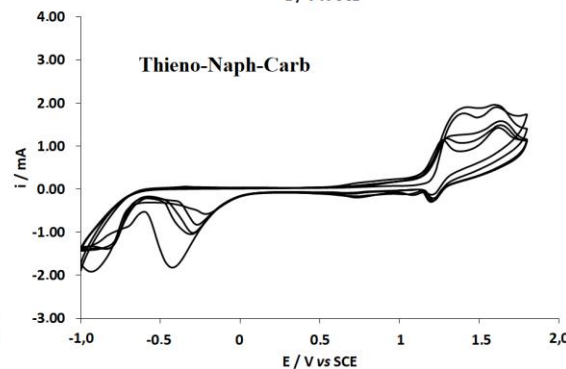
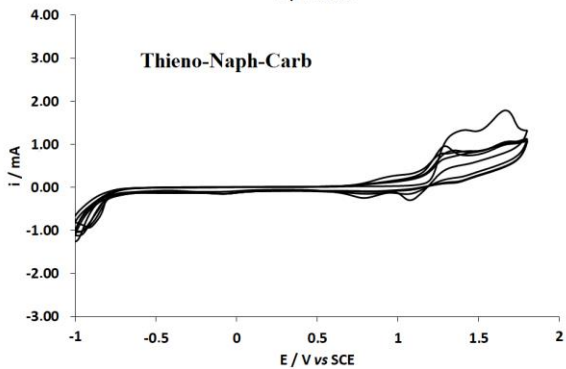
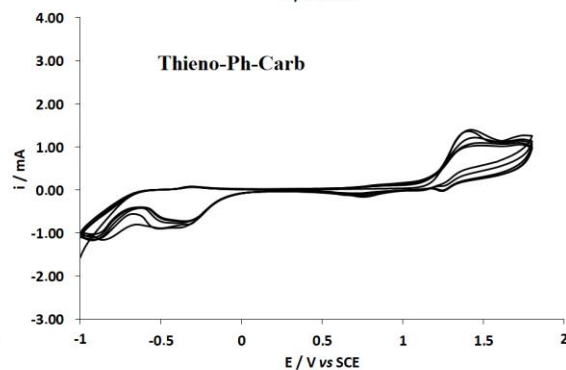
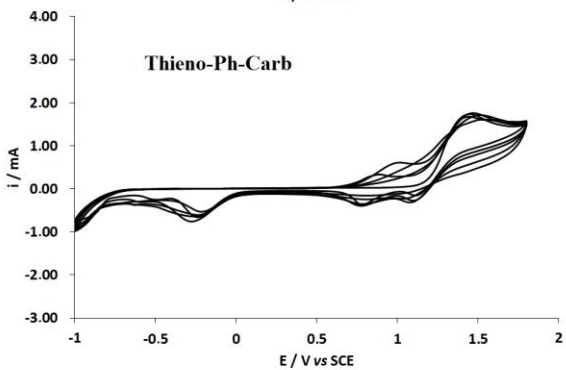
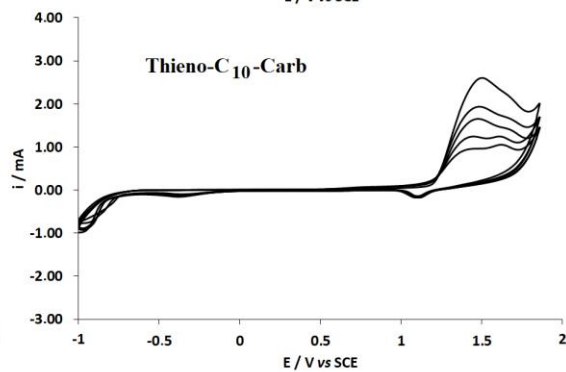
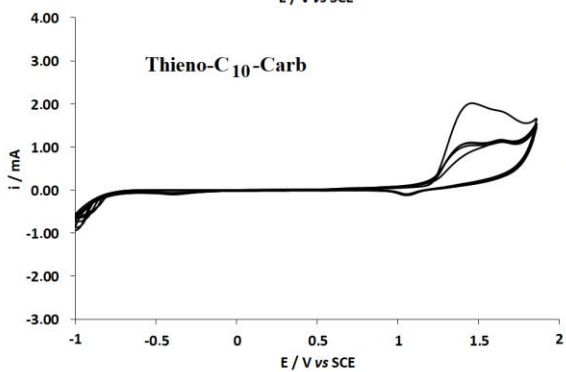
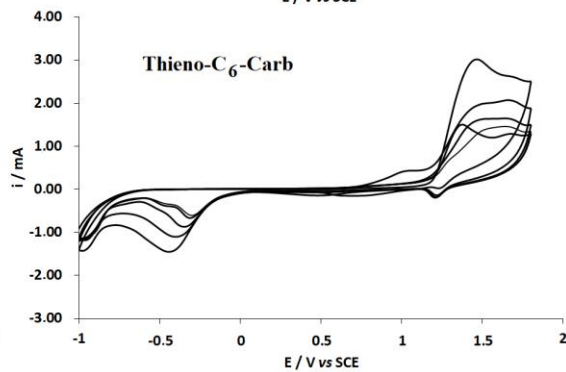
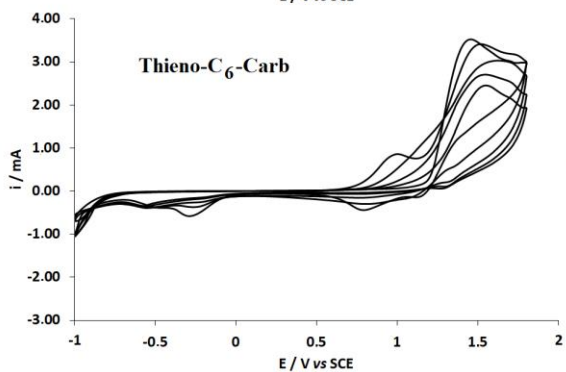
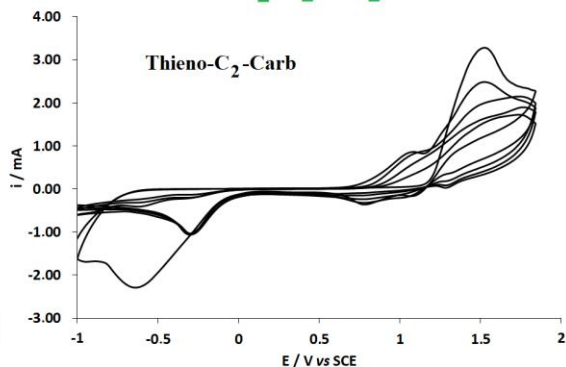


Figure 2. Electropolymerization of **Thieno-C₂-Carb**, **Thieno-C₆-Carb** and **Thieno-C₁₀-Carb**, **Thieno-Ph-Carb**, **Thieno-Naph-Carb** (10 mM) by cyclic voltammetry in 0.1 M Bu₄NClO₄ / CH₂Cl₂ (left) or CH₂Cl₂ + H₂O (right) at a scan rate 20 mV s⁻¹ (5 scans and $E = -1 / +E^{ox}$ V)).

3.2. Surface structures and wettability

Then, the surface morphology and wettability were characterized by SEM and goniometry. First of all, a huge difference in the presence of H₂O in the solvent used for electropolymerization is clearly observed with these monomers. In CH₂Cl₂, the surfaces are almost smooth even if some nanostructures are observed for example with **Thieno-C₄-Carb** and **Thieno-C₆-Carb** (Figure 3).

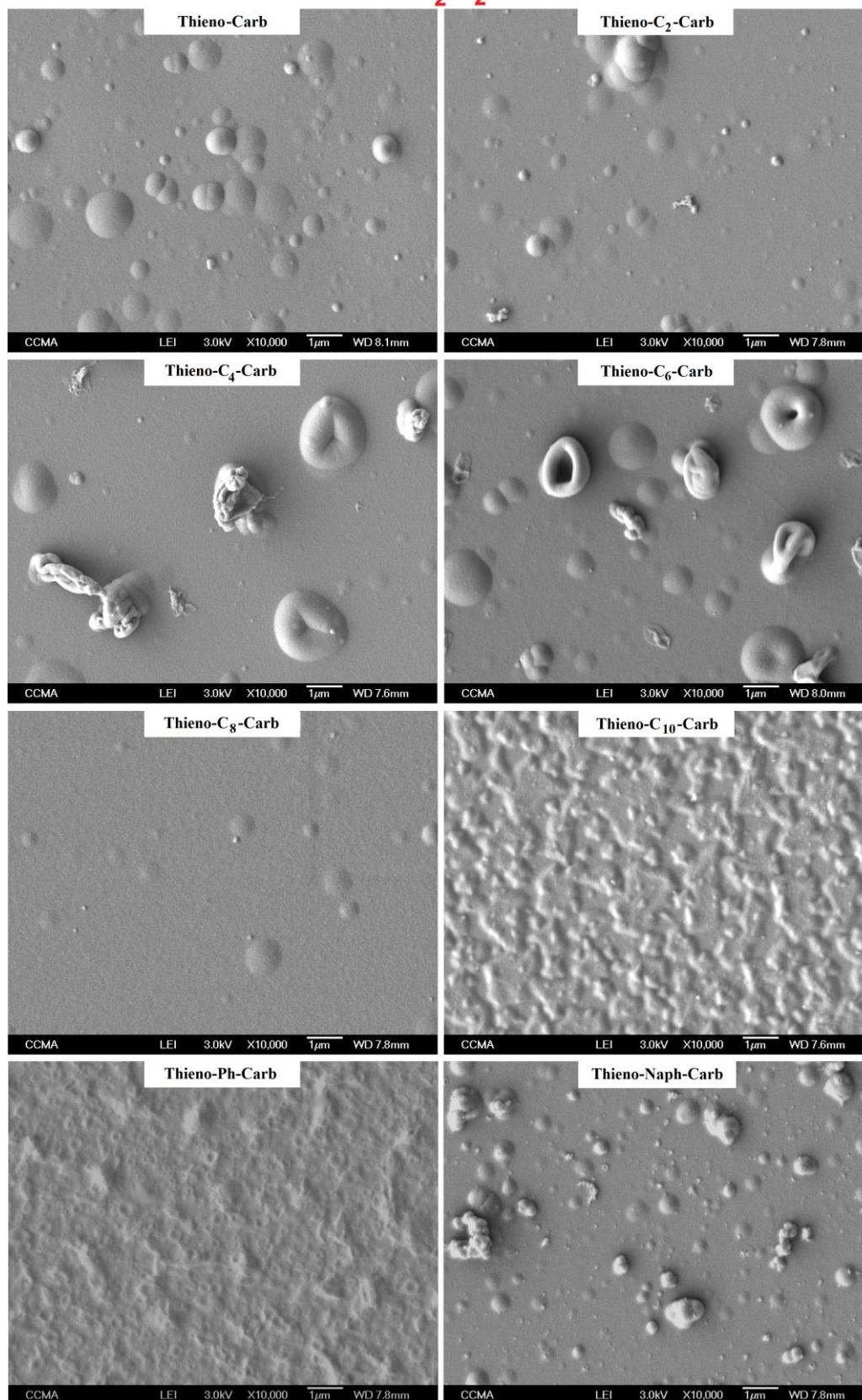


Figure 3. SEM images of the polymer surfaces electrodeposited from each monomer (10 mM) in 0.1 M $\text{Bu}_4\text{NClO}_4 / \text{CH}_2\text{Cl}_2$ in potentiodynamic conditions by cyclic voltammetry ($E = -1 / +E^{\text{ox}}$ V) after 3 scans. Magnification: $\times 10,000$.

In contrast, in $\text{CH}_2\text{Cl}_2 + \text{H}_2\text{O}$, a very nice change in the shape of the surface structures is clearly observed (Figure 4). Without alkyl spacer (**Thieno-Carb**), a huge number of nanoribbon-like structures is mainly observed indicating that the polymer growth is two-dimensional (2D). Similar structures are observed with very short alkyl spacer (Thieno-C₂-Carb) even if the surface is less rough. Using longer alkyl spacer ($\text{C}_2 < \text{C}_n < \text{C}_{10}$), the polymer growth changes. Here, the surfaces structures look like to nanorings indicating that the polymer growth is mainly in diameter and thickness rather than in height. Such structures were already rarely observed in the literature with this technique [41]. In order to better understand the influence of the alkyl spacer, we want to cite a publication [27] in which it was demonstrated that even the position of the substituent can highly affect the polymer growth. Due to different molecular stacking, PheDOT monomers with different the side groups (2-/1-naphthyl) led to different structures: mono-directionally growing (1D) vertically aligned nanotubes for 2Na-PheDOT and ribbon-like nanostructures (2D) for 1Na-PheDOT. Here, it is expected that the alkyl spacer would highly change the surface structures but the formation of nanorings is difficult to explain because three-dimensional (3D) structures are expected such as hollow spheres.

By doing supplementary SEM images but with inclination (Figure 5) the presence also of some nanoribbons except with **Thieno-C₈-Carb** for which almost only nanorings are observed with a diameter of $\approx 1 \mu\text{m}$, a thickness of $\approx 0.3 \mu\text{m}$ and a height of $\approx 0.4 \mu\text{m}$. With very long alkyl chains (C₁₀), porous structures are not observed because the polymer becomes too soluble in CH_2Cl_2 . Nanorings are observed whatever the number of deposition scan (tested done from 1 to 5 scans) as shown in Figure 6. From 1 to 3 scans, it is observed especially an increase in nanoring thickness and height (1 scan: diameter $\approx 1 \mu\text{m}$, thickness $\approx 0.2 \mu\text{m}$, height $\approx 0.2 \mu\text{m}$) while from 3 to 5 scans it is observed especially an increase of the number of nanorings but of various size. Here, even if there is a large dispersity it would be possible in the future to better control the homogeneity of the structures by doing the electrodepositions at constant potential, as observed in the literature for vertically aligned nanotubes [28,32,33]. Indeed, at constant potential only O₂ bubbles are released and it was observed that all the nanoseeds are formed in the first instance while the size of the structures is controllable with the deposition charge.

Using aromatic spacers (**Thieno-Ph-Carb** and **Thieno-Naph-Carb**), the surfaces are less structured even if a change from nanoribbon to nanoring structures is also observed but when the number of aromatic cycles is reduced.

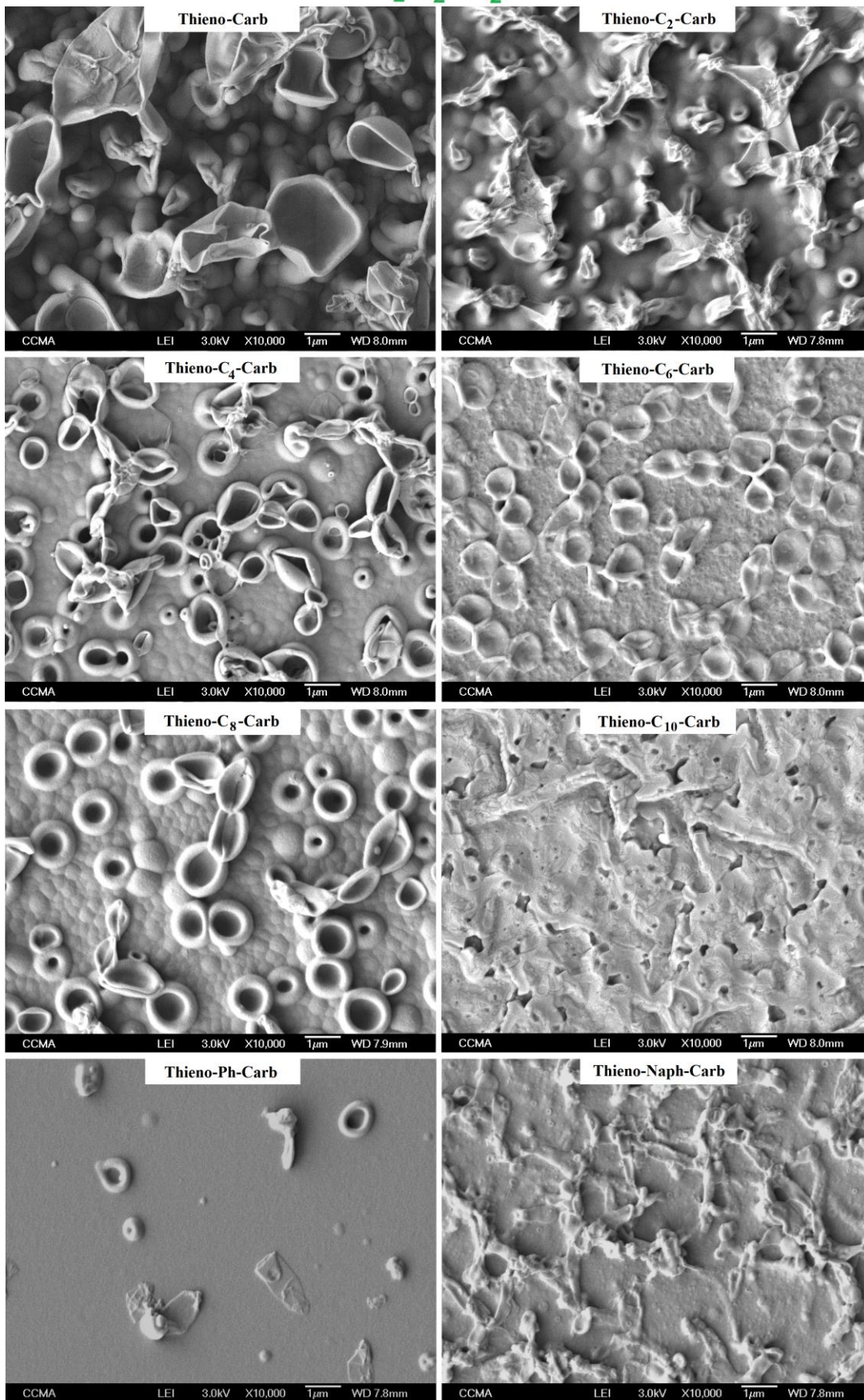


Figure 4. SEM images of the polymer surfaces electrodeposited from each monomer (10 mM) in 0.1 M Bu₄NClO₄ / CH₂Cl₂ + H₂O in potentiodynamic conditions by cyclic voltammetry ($E = -1 / +E^{ox}$ V) after 3 scans. Magnification: $\times 10,000$.

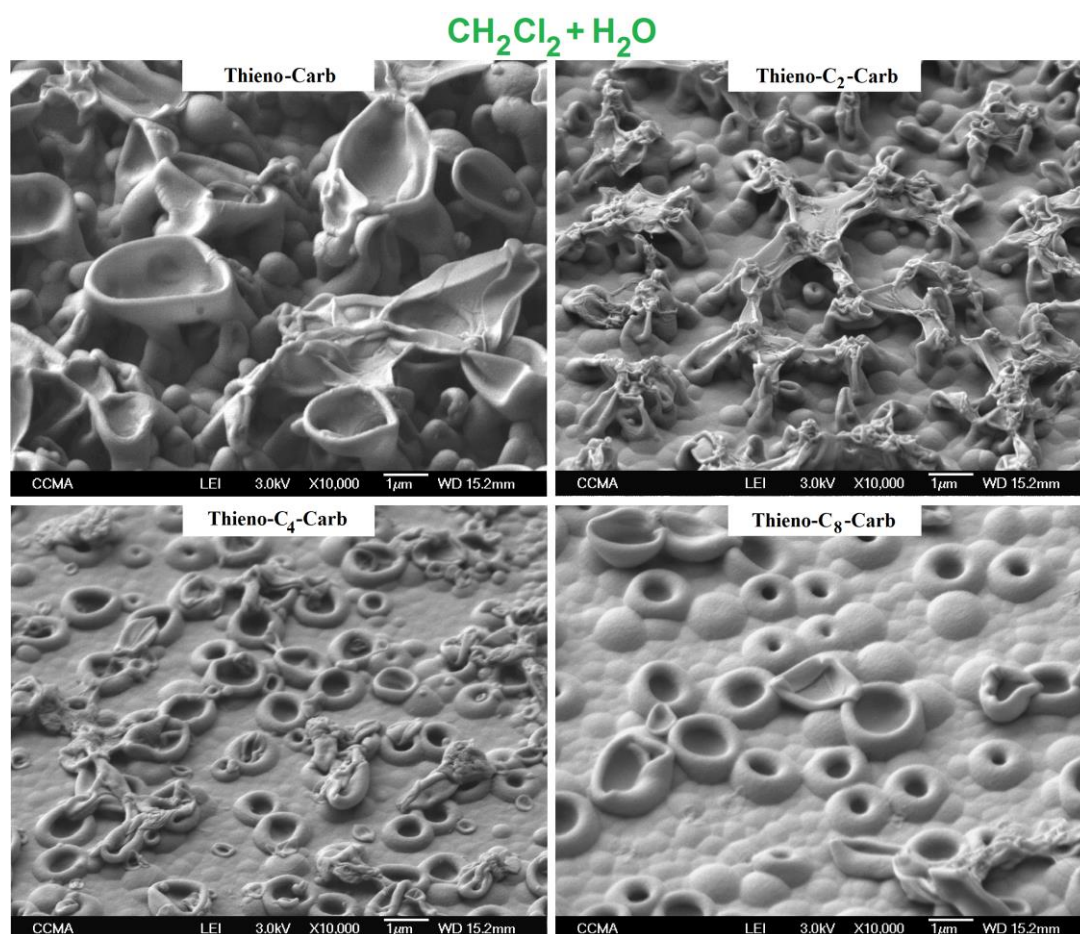
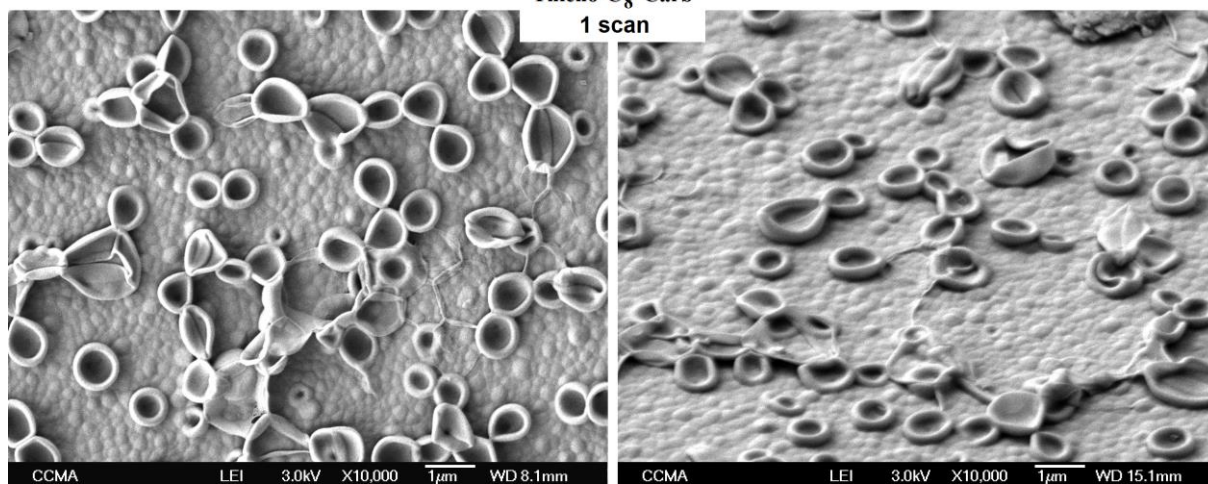


Figure 5. SEM images of the polymer surfaces electrodeposited from **Thieno-Carb**, **Thieno-C₂-Carb**, **Thieno-C₄-Carb** and **Thieno-C₈-Carb** (10 mM) in 0.1 M Bu₄NClO₄ / CH₂Cl₂ + H₂O in potentiodynamic conditions by cyclic voltammetry ($E = -1 / +E^{ox}$ V) after 3 scans. Magnification: $\times 10,000$. The substrates are inclined at 45°.

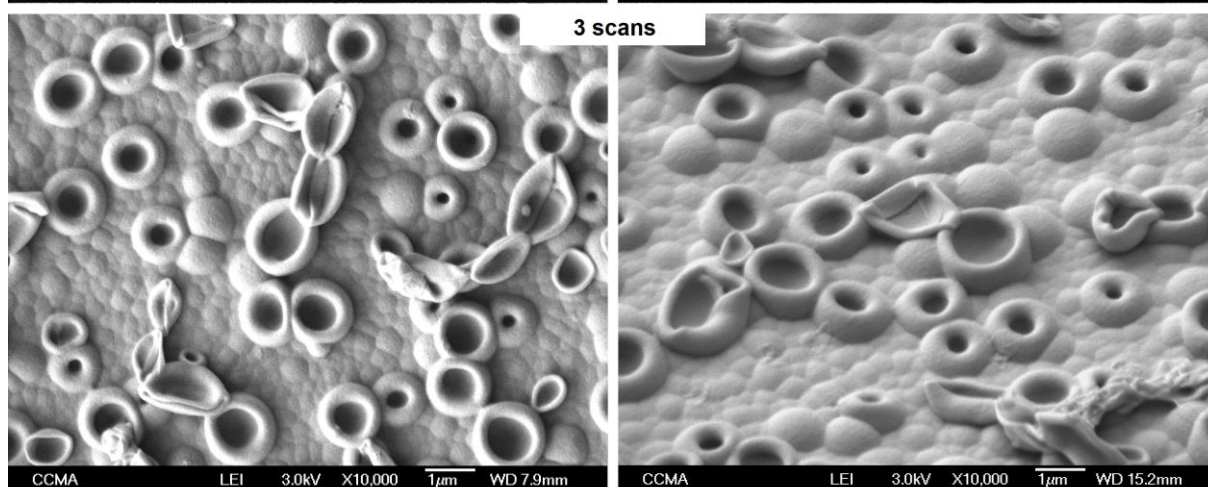


Thieno-C₈-Carb

1 scan



3 scans



5 scans

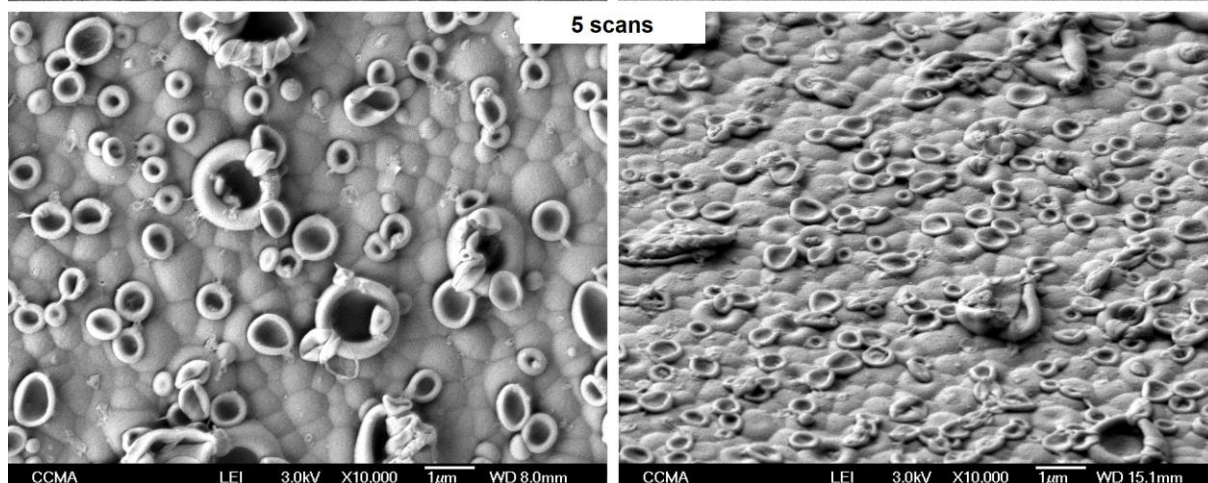


Figure 6. SEM images of the polymer surfaces electrodeposited from **Thieno-C₈-Carb** (10 mM) in 0.1 M Bu₄NClO₄ / CH₂Cl₂ + H₂O in potentiodynamic conditions by cyclic voltammetry ($E = -1 / +E^{ox}$ V) after 1, 3 and 5 scans. Magnification: $\times 10,000$. The substrates are not inclined (on the left) or inclined at 45° (on the right).

Their surface roughness and wettability were also determined. All the surfaces performed in CH₂Cl₂ (Table 1) are relatively smooth and all the polymers are intrinsically hydrophilic ($\theta_w < 90^\circ$). Here, it is normal that the surface hydrophobicity does not increase with the alkyl chain length because the alkyl chain is used as a spacer. For the surfaces performed in CH₂Cl₂ + H₂O (Table 2), they are structured but, here, it was not observed a significant increase in surface hydrophobicity. Indeed, because the polymers are intrinsically hydrophilic, it is necessary to trap a high amount of air inside between the surface and water droplet in order to increase the surface hydrophobicity (Cassie-Baxter equation). But here this is not the case for example with these nanorings because the surfaces are not very rough.

Table 1. Arithmetic and quadratic surface roughness (R_a and R_q) and wettability data for the polymer films obtained by cyclic voltammetry in in 0.1 M Bu₄NClO₄ / CH₂Cl₂ in potentiodynamic conditions by cyclic voltammetry ($E = -1 / +E^{ox}$ V) after 3 scans.

	R_a	R_q	θ_w
Monomer	[nm]	[nm]	[deg]
Thieno-Carb	72	93	87.2
Thieno-C₂-Carb	54	65	86.2
Thieno-C₄-Carb	17	26	85.7
Thieno-C₆-Carb	43	58	88.8
Thieno-C₈-Carb	40	55	84.3
Thieno-C₁₀-Carb	77	115	64.8
Thieno-Ph-Carb	14	17	77.9
Thieno-Naph-Carb	36	50	83.6

Table 2. Roughness (R_a and R_q) and wettability data for the polymer films obtained by cyclic voltammetry in 0.1 M $\text{Bu}_4\text{NClO}_4 / \text{CH}_2\text{Cl}_2 + \text{H}_2\text{O}$ in potentiodynamic conditions by cyclic voltammetry ($E = -1 / +E^{\text{ox}}$ V) after 3 scans.

	R_a	R_q	θ_w
Monomer	[nm]	[nm]	[deg]
Thieno-Carb	*	*	89.2
Thieno-C₂-Carb	78	118	82.4
Thieno-C₄-Carb	70	92	89.5
Thieno-C₆-Carb	40	52	85.5
Thieno-C₈-Carb	105	132	76.4
Thieno-C₁₀-Carb	170	220	61.9
Thieno-Ph-Carb	21	27	79.3
Thieno-Naph-Carb	30	38	60.3

*too rough for the apparatus

Finally, the films were also chemically analyzed. Example of infrared (IR) spectra obtained with **Thieno-C₈-Carb** and recorded by ATR are given in Figure 7. Peaks are present at $\approx 2800\text{-}3000 \text{ cm}^{-1}$ for C-H stretching as well as peak at 1708 cm^{-1} for C=O. Other peaks are present at $\approx 1050\text{-}1350 \text{ cm}^{-1}$ for example for C-O stretching.

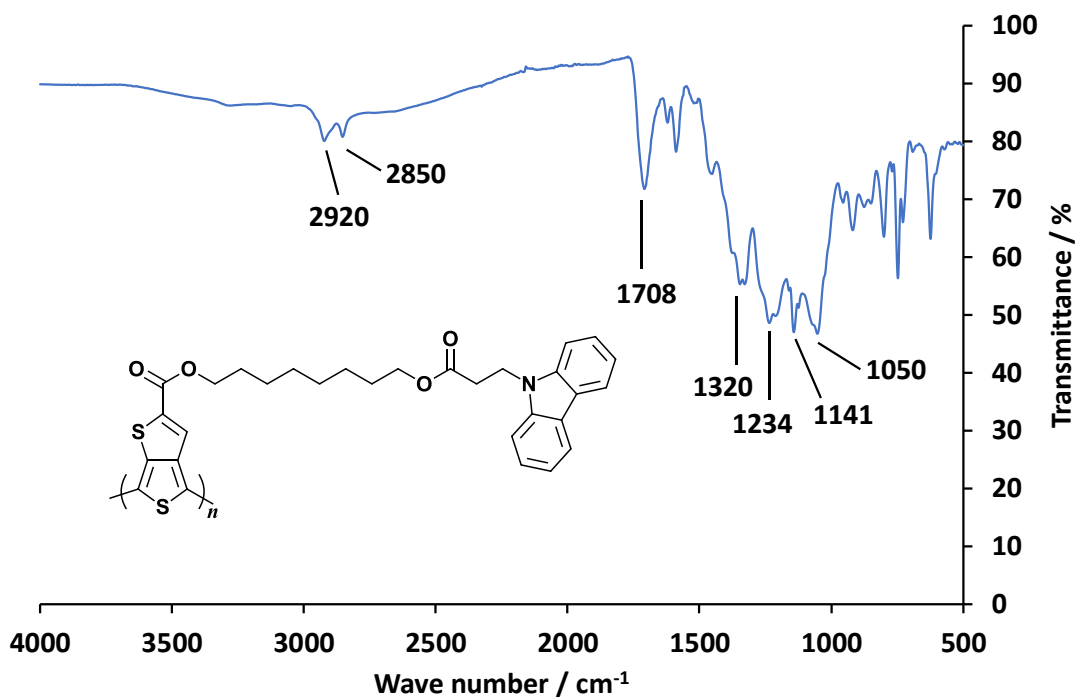


Figure 7. Infrared spectra of polymer surfaces obtained from **Thieno-C₈-Carb** *via* cyclic voltammetry (5 scans) and using CH₂Cl₂ as solvent.

The films were also chemically characterized by EDX. Very small peaks of the gold confirm the presence of gold on the substrate. Example of EDX spectra obtained with **Thieno-C₈-Carb** is shown in Figure 8. For the polymers, peaks characteristic of the presence of C, O and S are clearly present in the spectra with a much higher intensity for S peak. Moreover, very small peaks for Cl are also present, which may be due to the presence of some ClO₄⁻ counterions.

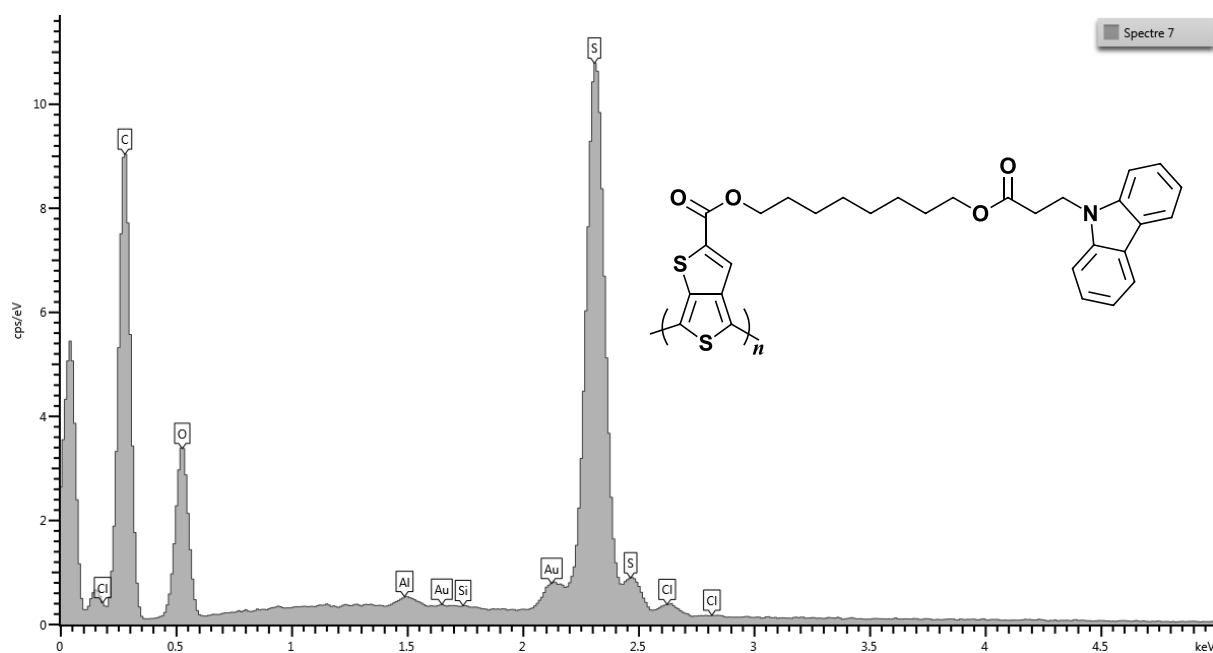


Figure 8. EDX spectra of polymer surfaces obtained from **Thieno-C₈-Carb** *via* cyclic voltammetry (5 scans) and using CH₂Cl₂ as solvent.

Conclusion

Here, we demonstrated the possibility to control the shape of the resulting porous structures by templateless electropolymerization. More precisely, we adjusted the spacer (alkyl chains or aromatic groups) between thieno[3,4-*b*]thiophene and carbazole used as the monomer and the substituent, respectively. A huge change was observed from ribbon-like structures to nanorings as the alkyl spacer increased but the presence of a significant amount of water was necessary in order to release a high amount of gas bubbles. It was possible to control the size and number of nanorings by the alkyl spacer and electrochemical parameters such as the number of deposition scans. These original materials could be applied in the future in various potential applications such as in water harvesting, oil/water separation membrane, optical devices, sensors or photocatalysis.

Acknowledgments

The group thanks Christelle Boscagli from the Centre Commun de Microscopie Appliquée (CCMA, Université Nice Sophia Antipolis) for the preparation of the substrates necessary for

the SEM analyses. The IR analyses were performed at the technological platform Smart City Innovation Center granted by Plan-Etat Region 2015–2020 (Provence-Alpes-Côte d'Azur).

References

- [1] T. Darmanin, F. Guittard, *Mater. Today* 18 (2015) 273–285.
- [2] W. Barthlott, M. Mail, B. Bhushan, K. Koch, *Nano-Micro Lett.* 9 (2017) 23.
- [3] L. Feng, Y. Zhang, J. Xi, Y. Zhu, N. Wang, F. Xia, L. Jiang, *Langmuir* 24 (2008) 4114–4119.
- [4] K. Liu, J. Du, J. Wu, L. Jiang, *Nanoscale* 4 (2012) 768–772.
- [5] B. Bhushan, M. Nosonovsky, *Phil. Trans. R. Soc. A* 368 (2010) 4713–4728.
- [6] A. Marmur, *Soft Matter* 8 (2012) 6867–6870.
- [7] Z. Cheng, J. Gao, L. Jiang, *Langmuir* 26 (2010) 11, 8233–8238.
- [8] H. Zhu, Z. Guo, W. Liu, *Chem. Commun.* 52 (2016) 3863–3879.
- [9] D. Chu, S.C. Singh, J. Yong, Z. Zhan, X. Sun, J.-A. Duan, C. Guo, *Adv. Mater. Interfaces* 6 (2019) 1900550
- [10] Y. Wang, X. Li, H. Hu, G. Liu, M. Rabnawaz, *J. Mater. Chem. A* 2 (2014) 8094–8102.
- [11] C. Hao, J. Li, Y. Liu, X. Zhou, Y. Liu, R. Liu, L. Che, W. Zhou, D. Sun, L. Li, L. Xu, Z. Wang, *Nat. Commun.* 6 (2015) 7986.
- [12] Q. Zhu, B. Li, S. Li, G. Luo, B. Zheng, J. Zhang, *Sci. Rep.* 9 (2019) 702.
- [13] L.Y. Yang, H.Z. Li, J. Liu, Z.Q. Sun, S. S. Tang, M. Lei, *Sci. Rep.* 5 (2015) 10908.
- [14] Z. Sun, T. Liao, K. Liu, L. Jiang, J.H. Kim, S.X. Dou, *Small* 10 (2014) 3001–3006.
- [15] S. Zhang, J. Huang, Y. Tang, S. Li, M. Ge, Z. Chen, K. Zhang, Y. Lai, *Small* 13 (2017) 1600687.
- [16] H.-A. Lin, S.-C. Luo, B. Zhu, C. Chen, Y. Yamashita, Y.-h. Yu, *Adv. Funct. Mater.* 23 (2013) 3212–3219.
- [17] A. Shumskaya, V. Bundyukova, A. Kozlovskiy, M. Zdorovets, K. Kadyrzhanov, G. Kalkabay, E. Kaniukov, *J. Magn. Magn. Mater.* 497 (2020) 165913.
- [18] M. Paulose, H.E. Prakasam, O.K. Varghese, L. Peng, K.C. Popat, G.K. Mor, T.A. Desai, C.A. Grimes, *J. Phys. Chem. C* 111 (2007) 14992–14997.
- [19] L. Lee, S.J. Park, *Chem. Rev.* 114 (2014) 7487–7556.
- [20] A. Fakhry, H. Cachet, C. Debiemme-Chouvy, *Electrochim. Acta* 179 (2015) 297–303.
- [21] C. Debiemme-Chouvy, A. Fakhry, F. Pillier, *Electrochim. Acta* 268 (2018) 66–72.

- [22] A. Fakhry, F. Pillier, C. Debiemme-Chouvy, *J. Mater. Chem. A* 2 (2014) 9859–9865.
- [23] L. Qu, G. Shi, J. Yuan, G. Han, F. Chen, *J. Electroanal. Chem.* 561 (2004) 149–156.
- [24] L. Qu, G. Shi, F. Chen, J. Zhang, *Macromolecules* 36 (2003) 1063–1067.
- [25] J.T. Kim, S.K. Seol, J.H. Je, Y. Hwu, G. Margaritondo, *Appl. Phys. Lett.* 94 (2009) 034103.
- [26] B. Parakhonskiy, D. Shchukin, *Langmuir* 31 (2015) 9214–9218.
- [27] T. Darmanin, E.L. Klimareva, I. Schewtschenko, F. Guittard, I.F. Perepichka, *Macromolecules* 52 (2019) 8088–8102.
- [28] C.R. Szczepanski, I. M’Jid, T. Darmanin, G. Godeau, F. Guittard, *J. Mater. Chem. A* 4 (2016) 17308–17323.
- [29] T. Darmanin, F. Guittard, *J. Mater. Chem. A* 4 (2016) 3197–3203.
- [30] S. Bai, Q. Hu, Q. Zeng, M. Wang, L. Wang, *ACS Appl. Mater. Interfaces* 10 (2018) 11319–11327.
- [31] O. Sane, A. Diouf, G. Morán Cruz, F. Savina, R. Méallet-Renault, S. Amigoni, S.Y. Dieng, F. Guittard, T. Darmanin, *Mater. Today* 31 (2019) 119–120.
- [32] I. Bousrih, M. El Kateb, C.R. Szczepanski, M. Beji, F. Guittard, T. Darmanin, *Phil. Trans. R. Soc. A* 378 (2020) 20190450.
- [33] M. Khodja, M. El Kateb, M. Beji, F. Guittard, T. Darmanin, *J. Colloid Interface Sci.* 564 (2020) 19–27.
- [34] S. Sow, A. Dramé, E.h.Y. Thiam, F. Orange, A. Sene, S.Y. Dieng, F. Guittard, T. Darmanin, *Prog. Org. Coat.* 138 (2020) 105382.
- [35] E.h.Y. Thiam, A. Dramé, S. Sow, A. Sene, C.R. Szczepanski, S.Y. Dieng, F. Guittard, T. Darmanin, *ACS Omega* 4 (2019) 13080–13085.
- [36] S. Bai, Q. Hu, Q. Zeng, M. Wang, L. Wang, *ACS Appl. Mater. Interfaces* 10 (2018) 11319–11327.
- [37] H. Wynberg, D.J. Zwanenburg, *Tetrahedr. Lett.* 8 (1967) 761–764.
- [38] G. Buemi, *Bull. Chem. Soc. Jpn.* 62 (1989) 1262–1268.
- [39] K. Lee, G.A. Sotzing, *Macromolecules* 34 (2001) 5746–5747.
- [40] Y. Wada, Y. Asada, T. Ikai, K. Maeda, T. Kuwabara, K. Takahashi, S. Kanoh, *ChemistrySelect* 1 (2016) 703–709.
- [41] A. Gbilimou, T. Darmanin, G. Godeau, F. Guittard, *ChemNanoMat* 4 (2018) 140–147.
- [42] M.-R. Azani, A. Hassanpour, *Chem. Eur. J.* 24 (2018) 19195–19199.

[43] P.S. Bols, H.L. Anderson, *Acc. Chem. Res.* 51 (2018) 2083–2092.

[44] X.Lin, Y. Liu, M. Lin, Q. Zhang, Z. Nie, *Chem. Commun.* 53 (2017) 10765–10767.

[45] J. Fang, J. Li, C. Tian, Q. Gao, X. Wang, N. Gao, X. Wen, C. Ma, H. You, Z. Yang, Q.-H. Xu, Q. Xiong, Z. Li, *NPG Asia Materials* 8 (2016) e323.

[46] T.H. Chow, Y. Lai, X. Cui, W. Lu, X. Zhuo, J. Wang, *Small* 15 (2019) 1902608.

Graphical Abstract

